EMBO
reports

scientific report

Structural basis for RNA-silencing suppression by *Tomato aspermy virus* protein 2b

Hong-Ying Chen[1]*, *Jing Yang*[2,3]*, *Chengqi Lin*[2] & *Y. Adam Yuan*[2,3]+

[1]Host–Pathogen Interaction Group, [2]Structural Biology Group, Temasek Life Sciences Laboratory, and [3]Department of Biological Sciences, National University of Singapore, Singapore

The 2b proteins encoded by *cucumovirus* act as post-transcriptional gene silencing suppressors to counter host defence during infection. Here we report the crystal structure of *Tomato aspermy virus* 2b (TAV2b) protein bound to a 19 bp small interfering RNA (siRNA) duplex. TAV2b adopts an all α-helix structure and forms a homodimer to measure siRNA duplex in a length-preference mode. TAV2b has a pair of hook-like structures to recognize simultaneously two α-helical turns of A-form RNA duplex by fitting its α-helix backbone into two adjacent major grooves of siRNA duplex. The conserved π-stackings between tryptophan and the 5′-terminal base of siRNA duplex from both ends enhance the recognition. TAV2b further oligomerizes to form a dimer of dimers through the conserved leucine-zipper-like motif at its amino-terminal α-helix. Biochemical experiments suggest that TAV2b might interfere with the post-transcriptional gene silencing pathway by directly binding to siRNA duplex.

Keywords: crystal structure; siRNA duplex recognition; RNA interference; viral suppressor

EMBO reports (2008) 9, 754–760. doi:10.1038/embor.2008.118

INTRODUCTION

RNA silencing is a small regulatory RNA-mediated biological process conserved in plants and animals (Tomari & Zamore, 2005; Patel *et al*, 2006; Hutvagner & Simard, 2008). In plants, RNA silencing is believed to be an ancient immune response triggered against viral double-stranded RNAs (dsRNAs; Ding & Voinnet, 2007). DsRNA molecules generating from viral RNAs are first recognized and processed by Dicer-like enzymes into small interfering RNA (siRNA) duplexes. The siRNA duplexes are then incorporated into an RNA-induced silencing complex (RISC) to target viral transcripts for degradation (Hutvagner & Simard, 2008). As a counter-defence strategy, many plant viruses have expressed suppressors to inhibit host RNA silencing by targeting different steps involved in siRNA pathway (Ding & Voinnet, 2007). It is speculated that dsRNA binding might be a general strategy to suppress RNA silencing in plants (Lakatos *et al*, 2006; Li & Ding, 2006), although other strategies exist (Zhang *et al*, 2006; Baumberger *et al*, 2007; Bortolamiol *et al*, 2007). Crystal structures of suppressors bound with dsRNA duplexes have provided the molecular details to understand the different suppression mechanisms adopted by different RNA-silencing suppressors. The crystal structure of *Tombusviral* P19 protein forms a head-to-tail homodimer to sequester siRNA duplex and prevents siRNA duplex loading into RISC (Vargason *et al*, 2003; Ye *et al*, 2003), whereas Flock House virus B2 protein forms a four-helix bundle homodimer to bind to dsRNA duplex regardless of length and prevents siRNA duplex formation as well as siRNA duplex loading into RISC (Chao *et al*, 2005; Lingel *et al*, 2005).

Cucumber mosaic virus protein 2b (CMV2b) is one of the first suppressors identified that could suppress host RNA silencing (Brigneti *et al*, 1998). Previously, we reported that CMV2b from the FNY strain interacted directly with *Arabidopsis* Argonaute1 (AGO1) *in vitro* and *in vivo* to inhibit RISC-mediated messenger RNA cleavage (Zhang *et al*, 2006). Recently, CMV2b from the CM95R strain was reported to bind to *in vitro*-synthesized siRNAs, indicating that CMV2b might suppress RNA silencing by binding directly to siRNAs (Goto *et al*, 2007). Similar to CMV2b, *Tomato aspermy virus* (also a member of the *cucumovirus* family) protein 2b (TAV2b) was reported to suppress RNA silencing (Lucy *et al*, 2000). Although TAV2b and CMV2b are homologues in their sequence, they vary widely in RNA-silencing suppression and resulting phenotype.

To define the molecular mechanism of TAV2b–dsRNA interaction and further compare the different RNA-silencing suppression mechanisms of TAV2b and CMV2b, we have determined the TAV2b (1–69) structure bound to a 19 bp siRNA duplex at 2.8 Å (TAV2b refers to TAV2b (1–69) hereafter). The structure shows that TAV2b interacts with a bound siRNA duplex through the deeply buried half of its protein segment inside the major groove of the siRNA duplex. TAV2b forms a pair of hook-like dimers to recognize the siRNA duplex in a sequence-independent and length-preference manner.

[1]Host–Pathogen Interaction Group, [2]Structural Biology Group, Temasek Life Sciences Laboratory, and [3]Department of Biological Sciences, National University of Singapore, 1 Research Link, Singapore 117604, Singapore
*These authors contributed equally to this work
+Corresponding author. Tel: +65 68727409; Fax: +65 68727007; E-mail: adam@tll.org.sg

Received 27 February 2008; revised 16 May 2008; accepted 20 May 2008; published online 4 July 2008

RESULTS

TAV2b is a small dsRNA-binding protein

We have confirmed by polyacrylamide gel electrophoretic mobility shift assay (EMSA) that TAV2b, which has sequence similarity with CMV2b, is able to bind to dsRNA. EMSA data show that TAV2b binds to both siRNA duplex (19 bp) and long siRNA duplex (30 bp) with a high binding affinity, whereas TAV2b binds to 26 nt dsDNA with a weak binding affinity (supplementary Fig S1 online).

TAV2b forms dimers in solution in the absence of dsRNA, which is confirmed by analytical gel filtration (Fig 1F; data not shown) and denatured SDS–PAGE (supplementary Fig S2 online). The dimeric form of TAV2b is extremely stable even when treated with SDS and boiled for 5 min. However, after the addition of dsRNA, the TAV2b–dsRNA complex migrates as a single peak at 60 kDa, which corresponds to a TAV2b–RNA tetramer (four TAV2b molecules and two dsRNA duplexes; Fig 1E,F).

Overview of the TAV2b–siRNA duplex complex structure

TAV2b adopts a novel fold and the structure contains two long α-helices connected by a conserved short link with half of its protein segment deeply buried within the major groove of the siRNA duplex. TAV2b forms a dimer and has a pair of hook-like structures to recognize the length of the siRNA duplex in a sequence-independent manner (Fig 1B,C). The long helical axes from the amino-terminal α1 helix and the carboxy-terminal α2 helix rotate 120° in relation to each other and are connected by a highly conserved linking region (Fig 1A). The long axis of N-terminal α1 is rotated 120° in relation to the siRNA duplex helical axis to maximize the interaction of the interface with the major groove, whereas the long axis of C-terminal α2 is almost parallel in relation to the siRNA duplex helical axis. TAV2b further dimerizes with its symmetrical related dimer by means of the conserved leucine-zipper-like motif (residues Leu 8, Ile 11, Leu 15 and Met 18) at its N-terminal α1 to form a dimer of dimers (Fig 1D), which is consistent with the analytical gel filtration experiment (Fig 1E,F). To investigate whether this tetramer also exists in solution, TAV2b protein was treated with EGS (ethylene glycol-bis) in the absence or presence of dsRNA. The EGS crosslinking data showed that TAV2b can be tetramerized and further oligomerized (supplementary Fig S2 online; data not shown). Importantly, EGS treatment of TAV2b mutants with the alanine substitutions on the leucine-zipper-like motif showed very weak oligomerization (supplementary Fig S2 online), which suggests that the tetramer observed at the crystal structure might also exist in solution. Notably, the mutations on leucine-zipper-like motif have no influence on dsRNA binding (Table 1; supplementary Fig S3A,B online).

Details of RNA–protein interactions

The TAV2b dimer buries 1,495 Å^2 of the total solvent-accessible area of the bound siRNA duplex, and almost all of the RNA–protein interactions are clustered along the continuous major groove of the bound siRNA duplex (Fig 2A,B). The hook-like two α-helical architecture of TAV2b forms a dimer to recognize two continuous helical turns formed by the 21 nt (19 bp) siRNA duplex by fitting the protein backbones into the major grooves (Fig 2B). At these locations, positively charged residues, such as invariable Arg 26, His 29, Asn 32, Arg 33 and Arg 36 from one surface of the TAV2b monomer, form hydrogen bonds and electrostatic interactions with both strands of the dsRNA (Fig 2A,B). Another patch of invariable residues, including Lys 39, Ser 40, Pro 41, Ser 42 and Glu 43, continuously form hydrogen bonds along the major groove (Fig 2B). The relatively conserved residue His 38 within the short link connecting the two α-helices further stabilizes the interactions by forming hydrogen bonds with the phosphate from the dsRNA, whereas the relatively conserved residue Gly 37 at this short link helps to kink the two long helical axes of TAV2b at an orientation of 120° to facilitate further the protein–RNA interactions. Interestingly, both Gly 37 and His 38 are conserved residues among the 2b family of proteins, with some exceptions—Cys substitution of Gly or Tyr substitution of His (Fig 1A). Nevertheless, the structural features of Cys and Gly (small side chain) or Tyr and His (aromatic ring and hydrogen bond) are conserved.

The invariable residue Pro 41 is located at the first residue of the C-terminal α-helix, the helical axis of which rotates 120° away from the helical axis of the N-terminal α-helix. The van der Waals interactions between the aromatic ring of Pro 41 and the phosphate moiety of uracil (U)15, together with the hydrogen bonds formed between its invariable neighbour residues Ser 40 and Ser 42 and the phosphorus atom of U15, further enhance the strong interactions between TAV2b and the siRNA duplex (Fig 2B). Thereby, the invariable residue Pro 41 has an important structural role to kink the protein and further anchor the C-terminal α-helix of TAV2b on the surface of the major groove of the bound siRNA duplex. In accordance with the structural observation, alanine mutation on residue Pro 41 decreased the dsRNA binding affinity ten times as shown by isothermal titration calorimetry assay (ITC; Table 1; supplementary Fig S3C online).

Remarkably, a unique tryptophan residue (Trp 50) projecting from the middle part of the C-terminal α-helix of one monomer π-stacks over the 5′-terminal base of the bound dsRNA from one side, whereas Trp 50 from its non-crystallographic symmetrical related molecule π-stacks over the 5′-terminal from the other side, thereby both ends of the siRNA duplex are recognized by the TAV2b dimer (Fig 2B). Although Trp 50 is relatively conserved, TAV2b might not strictly measure the length of siRNA duplex by this unique tryptophan residue. Our ITC data showed that the Trp50Arg mutant shows only two times less binding affinity, whereas the Trp50Ala mutant shows five times less binding affinity (Table 1; supplementary Fig S3E,F online).

Although there is no significant contribution to interaction from the 2′-OH group of RNA, TAV2b has the ability to distinguish between dsRNA and dsDNA by fitting its α-helical backbone into the major groove, thereby measuring the width of the major groove. In accordance with structural observations, ITC data show that the binding affinity between TAV2b and 26 nt dsDNA is 30 times lower than that between TAV2b and 21 nt dsRNA (Table 2; supplementary Fig S4A online), and the binding affinity between TAV2b and 12 nt dsRNA (12 bp) is about 30 times lower (Table 2; supplementary Fig S4B online). Moreover, ITC data further show that TAV2b binds to 21 nt single-stranded RNA at sequential binding sites with a weak binding affinity (~100 times lower; Table 2; supplementary Fig S4C online), and the binding affinity between TAV2b and 9 nt siRNA duplex (7 bp, no helical turn) is more than 150 times lower (Table 2; supplementary Fig S4D online). These data further confirm that TAV2b recognizes the dsRNA duplex by recognizing the helical turns.

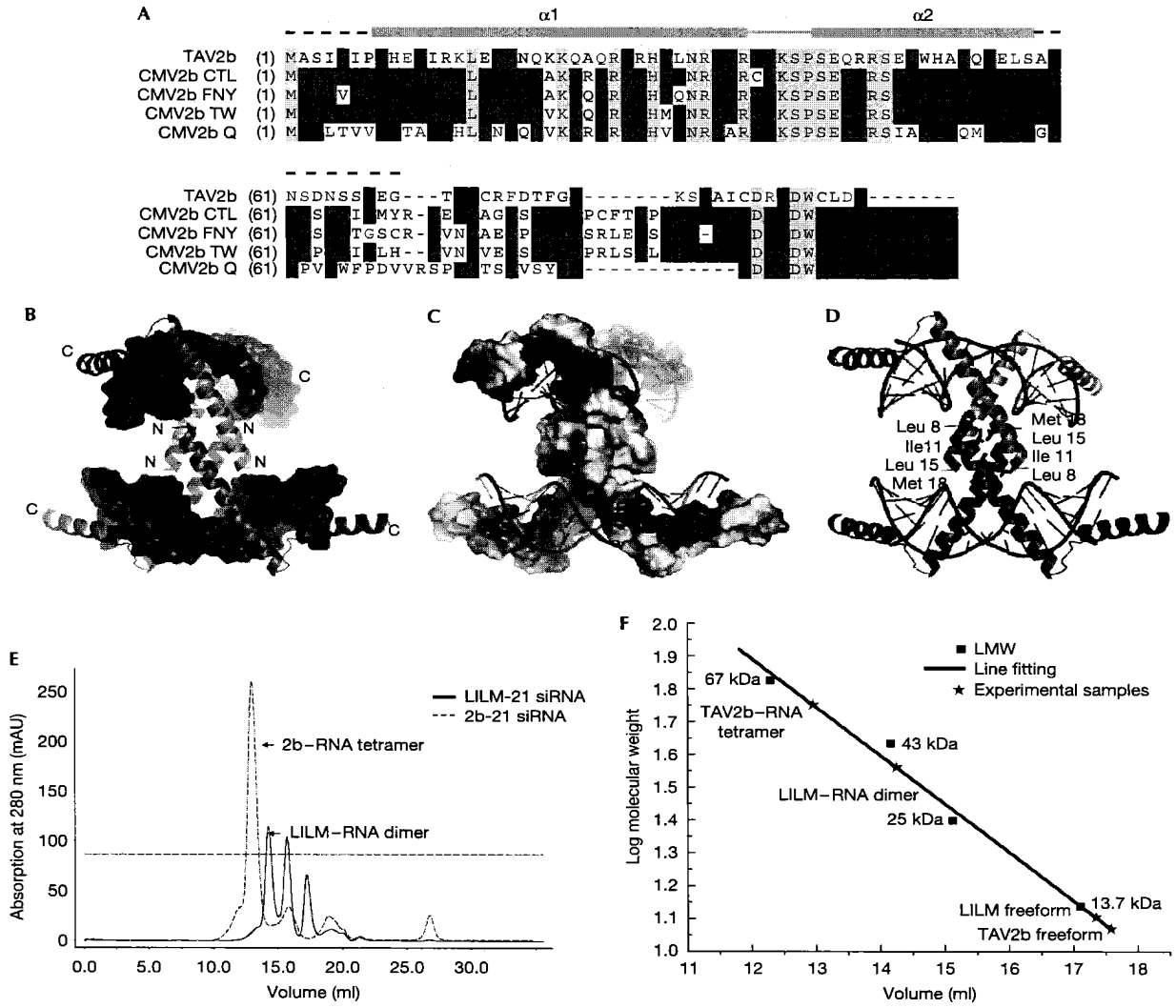

Fig 1 | Overall structure of the TAV2b–siRNA duplex complex. (**A**) Sequence alignment of 2b proteins from the *cucumovirus* family. A TAV2b protein comprising residues 1–69 was used in crystallization. Secondary elements in the X-ray structure are shown on the top. Dashed lines denote disordered residues. Conserved residues are shaded in cyan (80% conservation) and green (60% conservation), whereas essentially invariant residues are shaded in yellow. (**B**) TAV2b dimers are presented in a cartoon view and coloured in orange and magenta, whereas siRNA duplexes are represented in a surface view and coloured in cyan and green, respectively. (**C**) TAV2b dimers are presented in an electrostatic surface view with blue and red colours corresponding to positively and negatively charged patches, respectively, whereas siRNA duplexes are presented in a cartoon view and coloured in cyan and green, respectively. (**D**) Molecular details of protein–protein interactions. Cartoon representation of TAV2b–RNA tetramer with the conserved residues involved in leucine-zipper-like formation indicated. (**E**) Analytical gel filtration assays of TAV2b tetramerization. (**F**) Molecular-weight calculation aligned with the molecular standard. Structural figures were made by using PyMOL (http://pymol.sourceforge.net). CMV, *Cucumber mosaic virus* (strains CTL, FNY, TW and Q); LILM, Lys Ile Lys Met mutant; siRNA, small interfering RNA; TAV2b, *Tomato aspermy virus* 2b.

It was speculated that residues near the nuclear localization sites are crucial for RNA suppression by CMV2b (Lucy *et al*, 2000). Given the sequence similarity between CMV2b and TAV2b, we wonder whether these conserved residues at TAV2b are also crucial for dsRNA binding. RNA binding assay shows that mutations on the Arg28 and the invariable His29, which are adjacent to the proposed nuclear localization sites on the TAV2b sequence, decreased the RNA binding affinity by ten times (Table 1; supplementary Fig S3D online), which suggests that the weak binding affinity produced by the introduction of mutations might result in weak RNA-silencing suppression ability.

Table 1 | Binding of TAV2b and its mutants with a 21-nucleotide small interfering RNA duplex

	21-nucleotide small interfering RNA duplex					
$N = 0.5$	TAV2b (WT)	TAV2b (LILM Mut)	TAV2b (P41A Mut)	TAV2b (RH Mut)	TAV2b (W50R Mut)	TAV2b (W50A Mut)
K_d (M)	7.5×10^{-8}	8.0×10^{-8}	7.6×10^{-7}	8.4×10^{-7}	1.4×10^{-7}	3.4×10^{-7}
H (cal/mol)	-2.45×10^4	-3.135×10^4	-3.791×10^4	-3.305×10^4	-2.032×10^4	-1.672×10^4
S (cal/mol/deg)	−49.57	−72.68	−99.14	−83.06	−36.78	−26.49

LILM Mut, Lys Ile Lys Met mutant; Mut, mutant; TAV2b, *Tomato aspermy virus* 2b; WT, wild type.

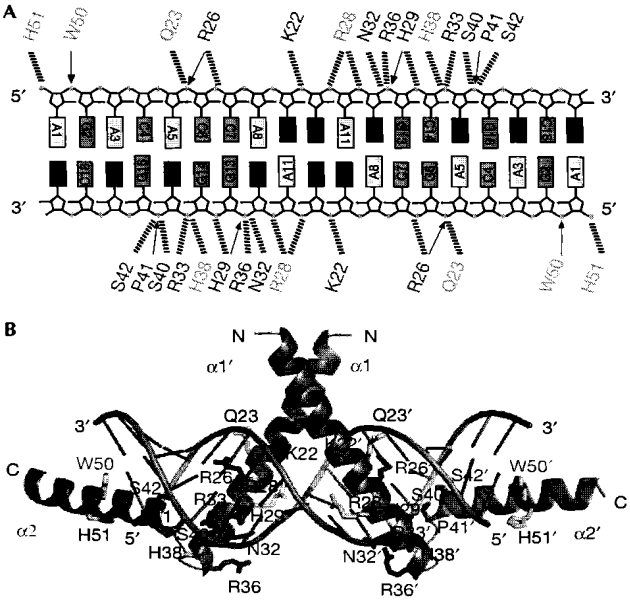

Fig 2 | Characterization of the RNA–protein interface and protein–protein interface of TAV2b. (A) Schematic representation of RNA–protein interactions. Dashed lines, hydrogen bonds with the phosphate backbone; solid arrows, van der Waals contacts. The invariable residues are coloured in red, whereas the relatively conserved residues are coloured in yellow. **(B)** Molecular details of RNA–protein interactions. One TAV2b–siRNA duplex represented in a cartoon view is shown for clarity. One TAV2b monomer is coloured in blue and another in green. The invariable residues are coloured in red, whereas the crucial Trp (W 50) residue is coloured in yellow. siRNA, small interfering RNA; TAV2b, *Tomato aspermy virus* 2b.

TAV2b suppresses RNA silencing

To test whether the key residues involved in siRNA duplex binding observed in the crystal structure are also involved in host RNA-silencing suppression, we performed *in vitro* RNA-silencing suppression experiments by *Agrobacterium* co-infiltration assay in transgenic plants that express green fluorescent protein (GFP). In these transgenic plants, GFP silencing can be triggered by transient GFP expression by *Agrobacterium* infiltration (Johansen & Carrington, 2001), whereas RNA-silencing suppressors, which initiate post-transcriptional gene silencing, can rescue transient expression of GFP in the infiltrated regions.

Our results show that transient expression of TAV2b suppressed GFP silencing and rescued the expression of GFP (Fig 3, lower left spot on each leaf), similar to suppression by the P19 proteins (Fig 3, upper right spot on each leaf; Siddiqui *et al*, 2008). As a negative control, GFP protein expression was almost completely suppressed when the GFP transgene was infiltrated alone (Fig 3, upper left spot on each leaf).

By contrast, single mutations on residue 50 (Trp50Arg and Trp50Ala) or residue 41 (Pro41Ala) and double mutations on residues 28 and 29 (Arg28AlaHis29Ala) showed a significant decrease in the expression level of GFP (Fig 3, lower right spot on each leaf), which suggests that RNA-silencing suppression ability of TAV2b is decreased after the introduction of point mutations. Although the mutation on Trp 50 has a rather small effect on binding *in vitro*, the effect on silencing is strong, which suggests that Trp 50 might contribute to further interactions with other proteins involved in the silencing pathway, such as AGO1. Nevertheless, the correlations of RNA binding affinity and RNA-silencing suppression ability shown by TAV2b mutants strongly suggest that TAV2b sequesters siRNA duplexes for RNA-silencing suppression.

DISCUSSION

TAV2b recognizes siRNA duplex by a pair of hook-like structures, which represents a distinct mode of dsRNA binding from previous structures of suppressor–dsRNA complexes. The viral p19 protein uses an extended β-sheet surface and a small α-helix to form a caliper-like architecture for binding and measuring the characteristic length of siRNAs (Fig 4A), whereas viral B2 protein uses a four-helical bundle fold to bind to both siRNA duplex and long dsRNA in a length-independent mode (Fig 4B). P19, B2 and all other known dsRNA-binding proteins recognize dsRNA by binding to only one face of the dsRNA to recognize the major or minor groove backbone (Fig 4A–C), whereas TAV2b recognizes dsRNA by fitting the protein backbones inside the major groove and wrapping around both faces of the dsRNA to recognize the major groove (Fig 4D).

Similar to viral B2 protein, TAV2b binds to both siRNA duplex and dsRNA, although TAV2b recognizes the 5′-terminal base of siRNA duplex by a relatively conserved tryptophan residue (Fig 4D). The promiscuous structural and functional deviation of dsRNA binding by TAV2b raises an interesting question regarding the physiological targets of TAV2b in host RNA-silencing suppression. It is possible that both dsRNA and siRNA duplex could be the targets of TAV2b, similar to viral B2 protein. This

Table 2 | RNA substrate recognition preference by TAV2b

	TAV2b wild type				
	26 nt dsDNA	**12 nt dsRNA**	**21 nt ssRNA**	**9 nt dsRNA**	**32 nt dsRNA**
N	0.361	0.811	Multiple sites	0.697	0.233
K_d (M)	2.1×10^{-6}	2.8×10^{-6}	NA	1.2×10^{-5}	1.4×10^{-7}
H (cal/mol)	4,905	-2.009×10^{4}	NA	7,221	-4.585×10^{4}
S (cal/mol/deg)	42.26	−42.00	NA	46.67	−122.4

dsRNA, double-stranded RNA; NA, not applicable; ssRNA, single-stranded RNA; TAV2b, *Tomato aspermy virus* 2b.

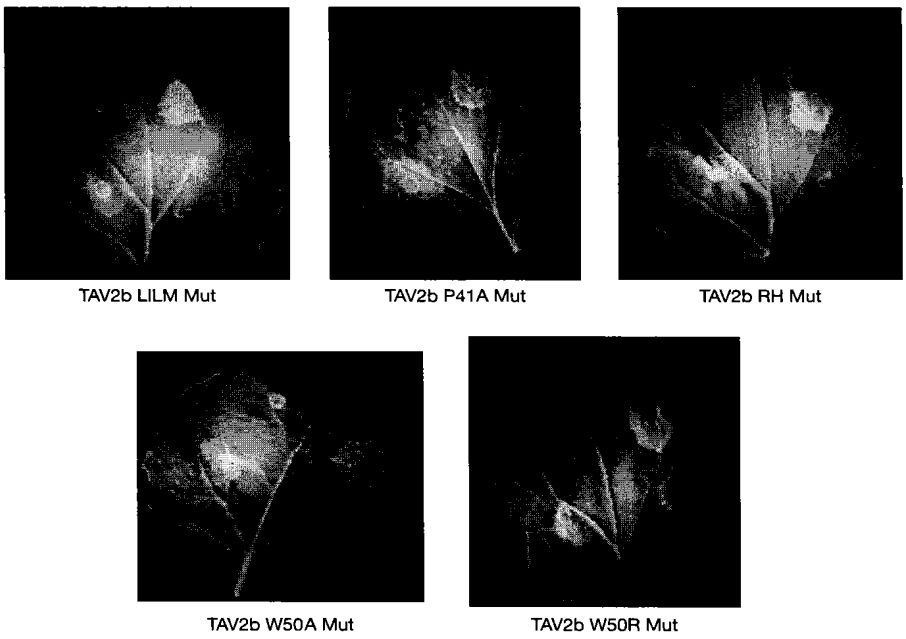

Fig 3 | RNA-silencing suppression in *Nicotiana benthamiana* by TAV2b. The GFP-expressing *N. benthamiana* leaves (C16) were co-infiltrated with a mixture of two *Agrobacterium tumefaciens* strains. One directs the expression of TAV2b wild type together with GFP (lower left spot on each leaf) and the other directs the expression of TAV2b mutant together with GFP (lower right spot on each leaf). The *A. tumefaciens* strain infiltrated with GFP expression vector was used as a negative control (upper left spot on each leaf), whereas *Tomato bushy stunt virus* p19 was used as a positive control (upper right spot on each leaf). The leaves were detached and photographed under UV illumination 6 days after infiltration. GFP, green fluorescent protein; LILM Mut, Lys Ile Lys Met mutant; TAV2b, *Tomato aspermy virus* 2b.

hypothesis is supported by our EMSA data and is in accordance with ITC data of TAV2b mutants at position Trp 50 (supplementary Fig S1 online; Table 1; supplementary Fig S3E,F online), but deviates from the structural observation of π-stacking between Trp 50 and the 5′-terminal base and *in vitro* RNA interference suppression data (Figs 2B, 3D,E). Although the extensive protein–dsRNA contacts can compromise the slight decrease in binding affinity induced by mutation of Trp 50, the functional role of Trp 50 is still unclear. At present, we cannot rule out the possibility that Trp 50 might have a role in the interaction between TAV2b and the proteins involved in the silencing pathway. Nevertheless, residue 50 is an invariable residue within CMV2b proteins and substituted by arginine in TAV2b protein (Fig 1A). The fact that arginine also can form π-stack contact with the base of RNA suggests that the π-stack contact observed in the crystal structure might have a physiological relevance. From the crystal structure, we noticed that the TAV2b dimer seems to accurately measure two helical turns of dsRNA by simultaneously recognizing two adjacent major grooves by its unique pair of hook-like structures. Our ITC analyses on the binding between TAV2b and different lengths of dsRNA showed that one TAV2b dimer recognizes two helical turns of dsRNA ($N = 0.5$). Theoretically, this recognition mode can also be applied to long dsRNAs by the simultaneous binding of many TAV2b dimers. The weak binding affinity

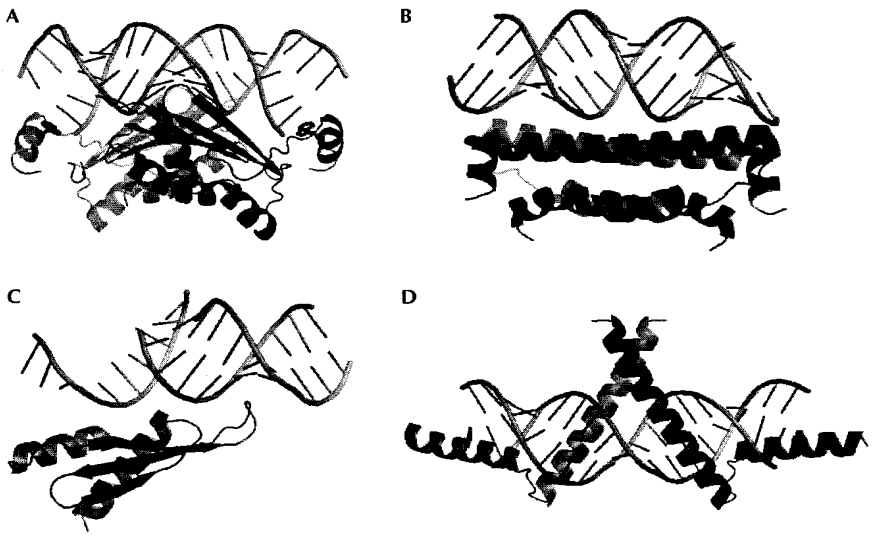

Fig 4 | Comparison of different dsRNA-binding modes between TAV2b and other RNA interference suppressors. (A) Cartoon view of the P19–siRNA duplex complex (Protein Data Bank (PDB) ID: 1R9F). **(B)** Cartoon view of the FHVB2–dsRNA complex (PDB ID: 2AZ0). **(C)** Cartoon view of the Xlrbpa2–dsRNA complex (PDB ID: 1DI2). **(D)** Cartoon view of the TAV2b–siRNA duplex complex (PDB ID: 2ZI0). dsRNA, double-stranded RNA; siRNA, small interfering RNA; TAV2b, *Tomato aspermy virus* 2b.

between TAV2b and long dsRNAs suggests that long dsRNAs might not be the preferred target of TAV2b (Shi *et al*, 2008). The conserved π-stack between 2b protein at residue 50 and dsRNA at the 5′-terminal base further suggests that TAV2b might prefer siRNA duplex instead of long dsRNA. In accordance with structural observations, ITC data show that TAV2b binds to 32 nt siRNA duplex (30 bp), which has three helical turns of dsRNA, with a binding affinity similar to that of 21 nt siRNA duplex (Table 2; supplementary Fig S4E online).

Previously, we reported that CMV2b was able to target *Arabidopsis* AGO1 to suppress host RNA silencing (Zhang *et al*, 2006). Here, we show that TAV2b, another member of the *cucumovirus* family, is able to bind directly to siRNA duplex to repress host RNA silencing. Taken together, the ability of *cucumovirus* 2b proteins to target both the RNA silencing trigger (siRNA) and the slicer (Argonaute) at the same time would provide an enormous advantage for the virus to survive during the arms race against the host (supplementary Fig S5 online).

METHODS

Protein purification and crystallization. The *TAV2b* gene was synthesized by a PCR-based approach and the recombinant TAV2b (residues 1–69) was generated by cloning into pET28b (Novagen; www.novagen.com) vector with a C-terminal His tag. Mutants of TAV2b were prepared using the QuikChange Site-Directed Mutagenesis Kit (Stratagene; www.stratagene.com). Recombinant TAV2b and its mutants were expressed in *Escherichia coli* (BL21/DE3 strain) overnight at 20 °C induced by 0.4 mM isopropyl β-D-thiogalactoside. Selenomethionine (Se-Met)-substituted TAV2b was prepared as described previously (Doublié, 1997). Proteins were purified through Ni^{2+} affinity column followed by HiLoad Superdex S-75 26/60 column. RNA oligoribonucleotides were purchased from Dharmacon (www.dharmacon.com). Crystals were grown at 20 °C by mixing 1.0 μl of protein–RNA complex (0.4 mM) with 1.0 μl of reservoir solution containing 25% PEG 1500, 1.0 M ammonium formate and 100 mM MES (pH 6.0), and equilibrated over 1 ml of reservoir solution for a course of 7 days.

Data collection and structure determination. Crystals were flash frozen (100 K) in the above reservoir solution supplemented with 30% glycerol. A two-wavelength data set was collected on a Se-Met crystal and processed by HKL2000 (www.hkl-xray.com). The structure was determined by multiwavelength anomalous dispersion using SHARP (www.globalphasing.com). The model was built by using the program O (http://xray.bmc.uu.se/alwyn) and refined using REFMAC/CCP4 (www.ccp4.ac.uk) with the crystallographic statistics listed in Supplementary Table 1 online. The model comprises residues 5–58. Disordered regions, including N-terminal tail 1–4, C-terminal tail 59–69 and 3′ dinucleotide overhangs of dsRNA, were not included in the model. The coordinates and the structure factors have been deposited in Protein Data Bank with accession code 2ZI0.

Analytical gel filtration. TAV2b proteins and protein–RNA complexes were analysed on Superdex 200 10/300 GL column with a flow rate of 0.5 ml/min and an injection volume of 0.1 ml. All the experiments were performed in a buffer of 25 mM Tris base and 100 mM NaCl (pH 7.4). For the complex, 2b and mutants were incubated with 21 nt dsRNA at the molar ratio of 1:1.1 on ice for 10 min. The column was calibrated by using the low-molecular-weight gel filtration kit (GE; www.ge.com) and the corresponding curves were established by OriginPro 7.5.

Isothermal titration calorimetry assay. All the experiments were performed in a buffer containing 12.5 mM Tris–HCl (pH 7.4) and 100 mM NaCl. Protein (20 μM) and RNA (200 μM) samples were filtered and degassed before titration. Protein samples were loaded into the cell and RNA samples were loaded into the syringe

with a stirring speed of 310 r.p.m. (Microcal VP-ITC calorimeter, Northampton, MA, USA). Data were collected in the high feedback mode with a filter period of 3 s. The calorimetric data were processed and fitted into the single set of identical sites model using Microcal Origin (version 5.0) and analysed by the software supplied with the instrument.

***Agrobacterium* co-infiltration assay.** TAV2b and its mutants were cloned into the pBA vector to generate constructs for infiltration, as described previously (Voinnet *et al*, 2000; Guo & Ding, 2002). These plasmids were then transformed into *Agrobacterium tumefaciens* strain EHA105 by electroporation and infiltrated into transgenic *Nicotiana benthamiana* expression GFP transgene (line 16C). The GFP fluorescence expression in *N. benthamiana* leaves was visualized by using a long-wave ultraviolet lamp (SB-100P/F high intensity ultraviolet lamp, Spectronics, USA; www.spectroline.com) and photographed by a Nikon D-80 digital camera with a yellow filter.

Supplementary information is available at *EMBO reports* online (http://www.emboreports.org).

ACKNOWLEDGEMENTS

We thank A. Saxena at X12C at the National Synchrotron Light Source of the Brookhaven National Laboratory for assistance with data collection, and N.-H. Chua and J. Ye for discussion. The coordinates and the structure factors have been deposited in Protein Data Bank with accession code 2ZI0. This work was supported by Temasek Life Sciences Laboratory and a research grant (T208A3124) from the Singapore Ministry of Education to Y.A.Y., who is a member of the Structural Biology and Proteomics Research Program supported by National University of Singapore.

CONFLICT OF INTEREST

The authors declare that they have no conflict of interest.

REFERENCES

Baumberger N, Tsai CH, Lie M, Havecker E, Baulcombe DC (2007) The Polerovirus silencing suppressor P0 targets ARGONAUTE proteins for degradation. *Curr Biol* **17:** 1609–1614

Bortolamiol D, Pazhouhandeh M, Marrocco K, Genschik P, Ziegler-Graff V (2007) The Polerovirus F box protein P0 targets ARGONAUTE1 to suppress RNA silencing. *Curr Biol* **17:** 1615–1621

Brigneti G, Voinnet O, Li WX, Ji LH, Ding SW, Baulcombe DC (1998) Viral pathogenicity determinants are suppressors of transgene silencing in *Nicotiana benthamiana*. *EMBO J* **17:** 6739–6746

Chao JA, Lee JH, Chapados BR, Debler EW, Schneemann A, Williamson JR (2005) Dual modes of RNA-silencing suppression by Flock House virus protein B2. *Nat Struct Mol Biol* **12:** 952–957

Ding SW, Voinnet O (2007) Antiviral immunity directed by small RNAs. *Cell* **130:** 413–426

Doublié S (1997) Preparation of selenomethionyl proteins for phase determination. *Methods Enzymol* **276:** 523–530

Goto K, Kobori T, Kosaka Y, Natsuaki T, Masuta C (2007) Characterization of silencing suppressor 2b of cucumber mosaic virus based on examination of its small RNA-binding abilities. *Plant Cell Physiol* **48:** 1050–1060

Guo HS, Ding SW (2002) A viral protein inhibits the long range signaling activity of the gene silencing signal. *EMBO J* **21:** 398–407

Hutvagner G, Simard MJ (2008) Argonaute proteins: key players in RNA silencing. *Nat Rev Mol Cell Biol* **9:** 22–32

Johansen LK, Carrington JC (2001) Silencing on the spot. Induction and suppression of RNA silencing in the *Agrobacterium*-mediated transient expression system. *Plant Physiol* **126:** 930–938

Lakatos L, Csorba T, Pantaleo V, Chapman EJ, Carrington JC, Liu YP, Dolja VV, Calvino LF, López-Moya JJ, Burgyán J (2006) Small RNA binding is a common strategy to suppress RNA silencing by several viral suppressors. *EMBO J* **25:** 2768–2780

Li F, Ding SW (2006) Virus counterdefense: diverse strategies for evading the RNA-silencing immunity. *Annu Rev Microbiol* **60:** 503–531

Lingel A, Simon B, Izaurralde E, Sattler M (2005) The structure of the flock house virus B2 protein, a viral suppressor of RNA interference, shows a novel mode of double-stranded RNA recognition. *EMBO Rep* **6:** 1149–1155

Lucy AP, Guo HS, Li WX, Ding SW (2000) Suppression of post-transcriptional gene silencing by a plant viral protein localized in the nucleus. *EMBO J* **19:** 1672–1680

Patel DJ, Ma JB, Yuan YR, Ye K, Pei Y, Kuryavyi V, Malinina L, Meister G, Tuschl T (2006) Structural biology of RNA silencing and its functional implications. *Cold Spring Harb Symp Quant Biol* **71:** 81–93

Shi BJ, Symons RH, Palukaitis P (2008) The cucumovirus 2b gene drives selection of inter-viral recombinants affecting the crossover site, the acceptor RNA and the rate of selection. *Nucleic Acids Res* **36:** 1057–1071

Siddiqui SA, Sarmiento C, Truve E, Lehto H, Lehto K (2008) Phenotypes and functional effects caused by various viral RNA silencing suppressors in transgenic *Nicotiana benthamiana* and *N. tabacum*. *Mol Plant Microbe Interact* **21:** 178–187

Tomari Y, Zamore PD (2005) Perspective: machines for RNAi. *Genes Dev* **19:** 517–529

Vargason JM, Szittya G, Burgyán J, Tanaka Hall TM (2003) Size selective recognition of siRNA by an RNA silencing suppressor. *Cell* **115:** 799–811

Voinnet O, Lederer C, Baulcombe DC (2000) A viral movement protein prevents spread of the gene silencing signal in *Nicotiana benthamiana*. *Cell* **103:** 157–167

Ye K, Malinina L, Patel DJ (2003) Recognition of small interfering RNA by a viral suppressor of RNA silencing. *Nature* **426:** 874–878

Zhang X, Yuan YR, Pei Y, Lin SS, Tuschl T, Patel DJ, Chua NH (2006) Cucumber mosaic virus-encoded 2b suppressor inhibits *Arabidopsis* Argonaute1 cleavage activity to counter plant defense. *Genes Dev* **20:** 3255–3268